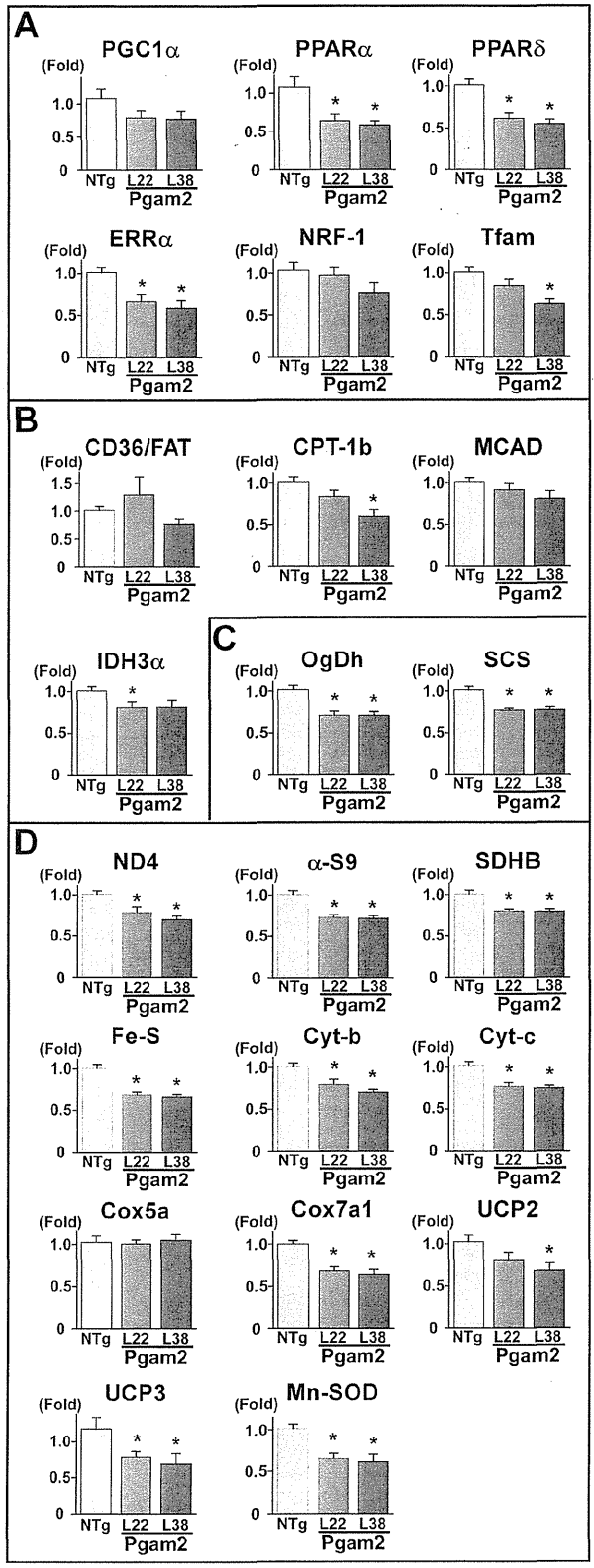

Figure 6. The expression of genes related to mitochondria was decreased in Pgam2 mice. The expression of genes related to mitochondria was analyzed using quantitative real-time PCR. The genes presented here are involved in **(A)** transcriptional regulators, **(B)** fatty acid metabolism, **(C)** the TCA cycle, and **(D)** mitochondria. Peroxisome proliferator-activated receptor α (PPARα), peroxisome proliferator-activated receptor δ (PPARδ), estrogen related receptor α (ERRα), mitochondrial transcription factor A (Tfam), carnitine palmitoyltransferase 1b (CPT-1b), isocitrate dehydrogenase 3 α (IDH3α), oxoglutarate dehydrogenase (OgDh), succinyl-CoA synthetase α (SCS), mitochondrially encoded NADH dehydrogenase 4 (ND4), alpha-subcomplex 9 of complex I (α-s9), mitochondrial succinate dehydrogenase iron-sulfur subunit (SDHB), iron-sulfur protein (Fe-S), cytochrome b (Cyt-b), cytochrome c (Cyt-c), cytochrome c oxidase subunit VIIa (COX7a), uncoupling protein 2 (UCP2), uncoupling protein 3 (UCP3), and manganese superoxide dismutase (Mn-SOD) levels were decreased in Pgam2 mice. NRF-1: nuclear respiratory factor 1; CD36/FAT: CD36/fatty acid translocase; MCAD: medium-chain acyl coenzyme A dehydrogenase; Cox5a: mitochondrial cytochrome c oxidase subunit Va. The amount of target gene mRNA was normalized by 18S rRNA mRNA. Values are the mean ± SEM. Gene expression levels in Pgam2 mice were compared with those of NTg mice. *$p<0.05$ versus NTg mice ($n=12$ for each group).
doi:10.1371/journal.pone.0072173.g006

weight (LW)/body weight ratio (LW/BW) of Pgam2 mice was also higher than that of NTg mice with TAC (Figure 9B), which suggested the presence of pulmonary congestion in Pgam2 mice with TAC. Fibrosis was not observed with Sirius Red staining in Pgam2 mice with the sham operation. However, the fibrotic area in Pgam2 mice with TAC was significantly larger than that of NTg mice with TAC (Figure 9C). Thus, Pgam2 mice developed heart failure associated with enhanced cardiac hypertrophy and fibrosis.

We then examined the expression of genes related to mitochondria in NTg and Pgam2 mice under sham and TAC operations. The expression of several genes related to mitochondria was decreased in NTg mice with TAC (Figure 10A-D). Pgam2 overexpression further decreased the expression of some genes, such as ERRα, Tfam, medium-chain acyl coenzyme A dehydrogenase (MCAD), Cox5a, and Cox7a1, in response to TAC (Figure 10A-D).

Discussion

We examined the effects of the persistent overexpression of Pgam2 on energy metabolism and stress resistance in the heart in this study. Cardiac function at rest was normal. Uptake of the analogs of glucose and a fatty acid, and the PCr/βATP ratio at rest were normal in Pgam2 mice. However, the persistent overexpression of Pgam2 altered the levels of metabolites involved in glycolysis and the TCA cycle, and the expression of genes related to mitochondrial function at baseline. The capacity for mitochondrial respiration decreased, and that for mitochondrial ROS production increased in *in vitro* experiments using isolated mitochondria. Pgam2 mice developed systolic dysfunction upon dobutamine infusion and pressure overload.

The Pgam protein in Pgam2 mice with TAC was 6.9-fold higher than that in NTg mice with TAC. Pgam protein levels in Pgam2 mice with TAC were lower than those in Pgam2 mice with the sham operation, which may have been due to reduced α-MHC promoter activity upon TAC [40]. Pgam2 mice with the sham operation showed preserved cardiac function. Cardiac function in NTg mice with TAC was preserved. However, Pgam2 mice with TAC showed decreased systolic function and increased lung weight, which indicated the development of heart failure. Pgam protein levels were shown to increase by approximately 5-fold in a canine model of heart failure [24]. Thus, increased Pgam protein levels were involved in the development of heart failure under stressed conditions.

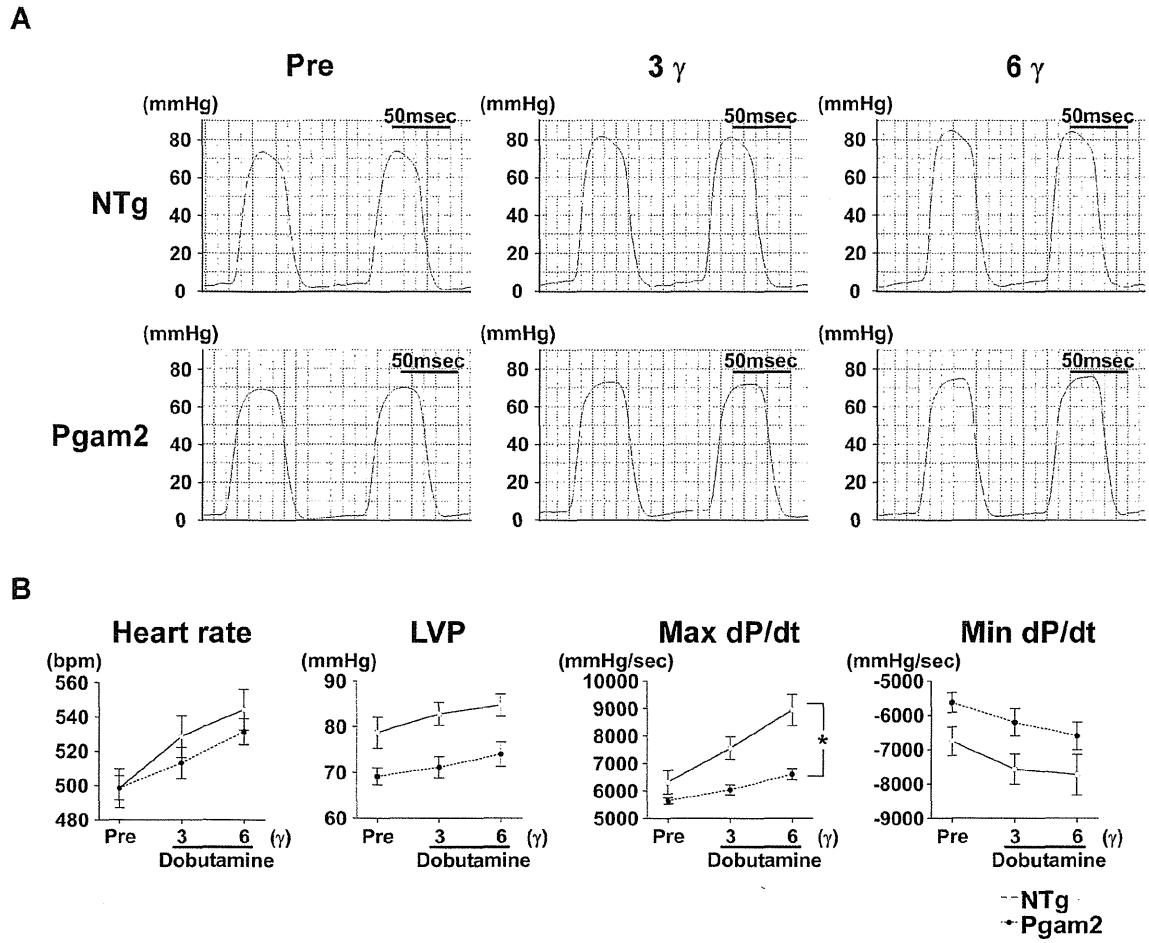

Figure 7. Cardiac function in response to dobutamine was impaired in Pgam2 mice. Cardiac function was analyzed by cardiac catheterization under dobutamine infusion. (**A**) Representative traces of left ventricular pressures. (**B**) Cardiac systolic function in response to dobutamine was impaired in Pgam2 mice. LVP: left ventricular systolic pressure; γ: μg/kg/min. A two-way repeated-measures ANOVA was used to test differences between groups in response to dobutamine infusion. Values are the mean ± SEM. *$p<0.05$, interaction of dobutamine doses with differences between Pgam2 mice and NTg mice (n = 10 for each group).
doi:10.1371/journal.pone.0072173.g007

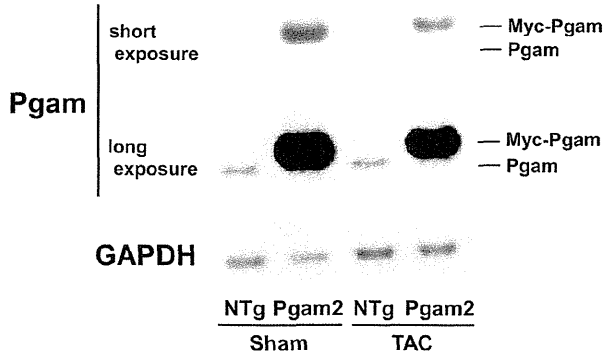

Figure 8. Pgam protein in NTg or Pgam2 mice with the sham or TAC operation. A representative western blot of NTg or Pgam2 mice with the sham or transverse aortic constriction (TAC) operation.
doi:10.1371/journal.pone.0072173.g008

Pgam2 overexpression in primary mouse embryonic fibroblasts (MEFs) increased the production of ^3H_2O from [3-^{3}H]glucose and lactate production, which indicates that glycolytic flux is increased

Table 3. Expression of the Pgam protein in NTg or Pgam2 mice with the sham operation or transverse aortic constriction.

	Sham		TAC	
	NTg	Pgam2	NTg	Pgam2
	(n = 4)	(n = 4)	(n = 4)	(n = 4)
Pgam/GAPDH	1.0 ± 0.4	13.1 ± 2.3†	0.7 ± 0.1	4.6 ± 0.6*†

Values are expressed as the mean ± SEM. NTg: non-transgenic mice; Pgam2: phosphoglycerate mutase 2 transgenic mice; TAC: transverse aortic constriction. The mean value of NTg mice with the sham operation was used as a standard. *$p<0.05$ versus the same genotype with the sham operation. †$p<0.05$ versus NTg mice with the same operation.
doi:10.1371/journal.pone.0072173.t003

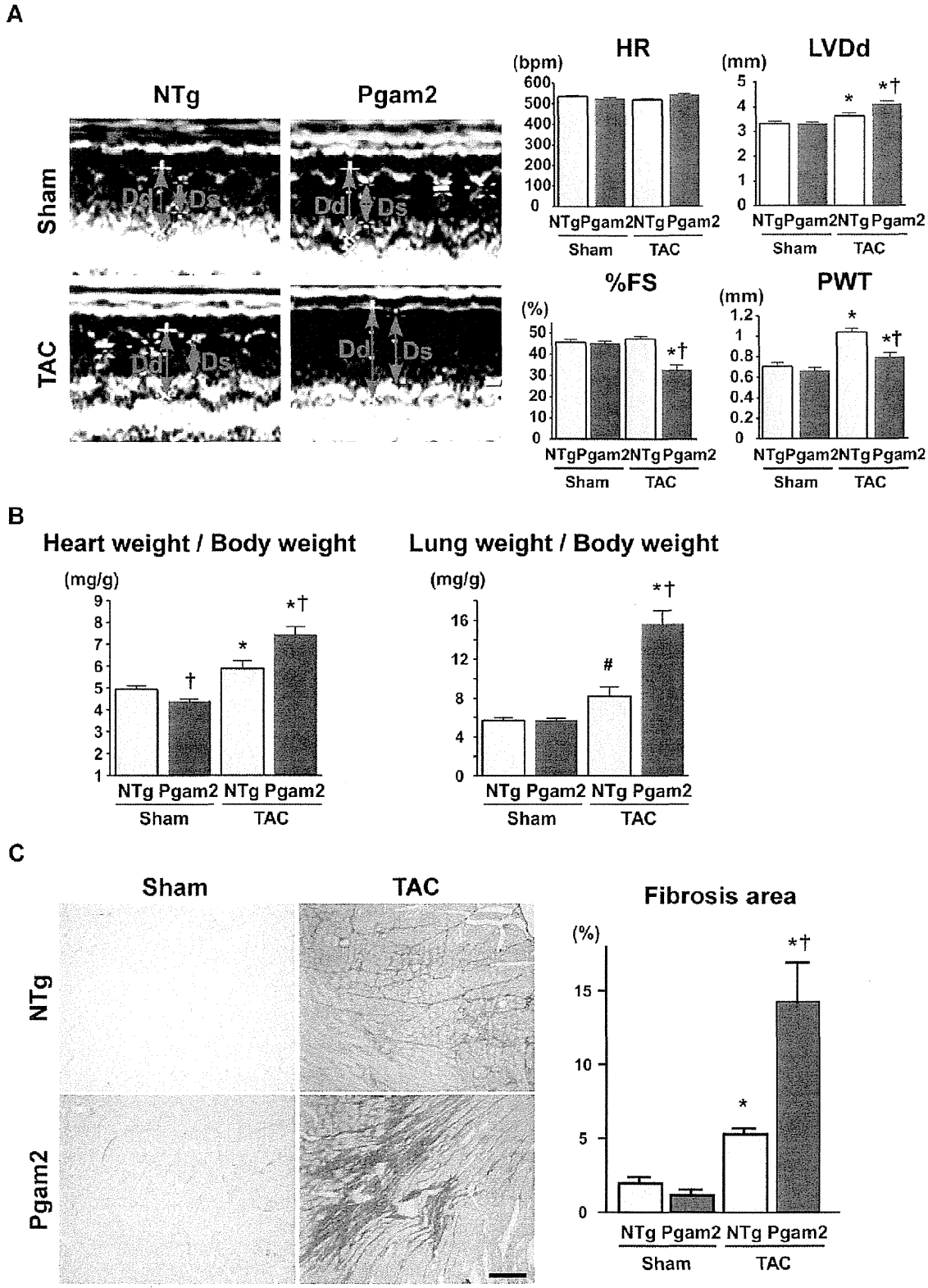

Figure 9. Pgam2 mice developed systolic dysfunction and myocardial fibrosis in response to pressure overload. (A) A representative M-mode echocardiogram is shown in the left panel. The left ventricular end-diastolic dimension (LVDd) was higher and %FS was lower in Pgam2 mice with TAC than in NTg mice with TAC. Dd: LVDd; Ds: left ventricular end-systolic dimension; HR: heart rate; bpm: beats per minute; FS: fractional

shortening; PWT: posterior wall thickness. (B) The heart weight/body weight ratio and lung weight/body weight ratio of Pgam2 mice were higher than those of NTg mice with TAC. (C) Myocardial fibrosis was analyzed using Sirius Red staining. The ratio of the fibrotic area to the whole short-axis sectional area was calculated. Myocardial interstitial fibrosis was observed in NTg mice with TAC. Myocardial fibrosis was enhanced in Pgam2 mice with TAC. Values are the mean ± SEM. *$p<0.05$ versus the same genotype with the sham operation. †$p<0.05$ versus NTg mice with the same operation. # $p=0.08$ vs NTg mice with the sham operation. Sham-operated NTg mice: n = 6; sham-operated Pgam2 mice: n = 4; NTg mice with TAC: n = 8; Pgam2 mice with TAC: n = 6.
doi:10.1371/journal.pone.0072173.g009

[18]. Although we did not measure the actual glycolytic flux, we suggest that it was not changed in Pgam2 hearts for the following reasons. First, uptake of the glucose analog and G6P was not changed, which indicates that the level of glucose that enters the glycolytic pathway may not be changed. Second, although the levels of metabolites just upstream and downstream of Pgam were changed, those in the initial steps of glycolysis and of lactate, an end product of glycolysis, remained unchanged. The intermediary metabolites of glycolysis, such as 3PG, 2PG, and PEP, were shown to be increased, and 3PG, 2PG, and PEP have been reported to inhibit PFK activity in plants [38]. Indeed, PFK activity was decreased and may have canceled the increase in Pgam enzymatic activity. The decrease in the gene expression of the rate-limiting enzymes of glycolysis may have also attenuated the booster effects of Pgam2 overexpression on glycolytic flux. The different effects of Pgam2 overexpression on glucose metabolism in MEFs and murine hearts may be due to metabolic differences between cultured fibroblasts and intact heart tissue.

The major biological function of mitochondria is ATP synthesis via oxidative phosphorylation. In addition, mitochondria play an important role in various cellular functions including redox homeostasis, calcium regulation, apoptosis, and the synthesis and catabolism of metabolites. A number of *in vitro* and *in vivo* methods have been used to examine the various functions of mitochondria, and have advantages and limitations [41,42]. The capacity for ROS generation measured *in vitro* using isolated mitochondria was increased, while TBARS, a marker of ROS measured *in vivo*, did not change in Pgam2 mice. Mitochondrial morphology was also normal on electron microscopic analysis. Differences in the markers of ROS between *in vitro* and *in vivo* analyses may be explained by other cellular factors that may have regulated the mitochondrial functions observed *in vivo*, over those observed *in vitro*. In addition, the abnormal functions of isolated mitochondria in the presence of normal mitochondrial morphology have been previously reported [43]. We speculate that, in spite of relatively normal morphology, persistent Pgam2 overexpression perturbed some of the functions of mitochondria and increased susceptibility to stress.

The mechanism by which Pgam2 overexpression impairs mitochondria is unknown and requires further investigation. However, Pgam2 overexpression also reduces mitochondrial respiration in MEFs [44]. One possibility is that the accumulation of glycolytic and TCA cycle intermediates caused mitochondrial dysfunction. Phosphoenolpyruvate (PEP) was shown to inhibit mitochondrial respiration [45], and was 2.3-fold higher in Pgam2 mice. Mitochondrial complex II is composed of ubiquinone oxidoreductase and succinate dehydrogenase (SDH), which oxidizes succinate to fumarate, reduces ubiquinone, and connects the TCA cycle and mitochondrial respiration. TCA cycle intermediates are known to regulate complex II activity and ROS generation [46]. Amino acids have also been shown to regulate mitochondrial function. The depletion of endogenous GSH increased mitochondrial ROS [47] and decreased mitochondrial respiration [48]. Aspartate and betaine protected cardiac mitochondrial function in a rat model of myocardial infarction [49,50]. Proline and betaine were also shown to protect

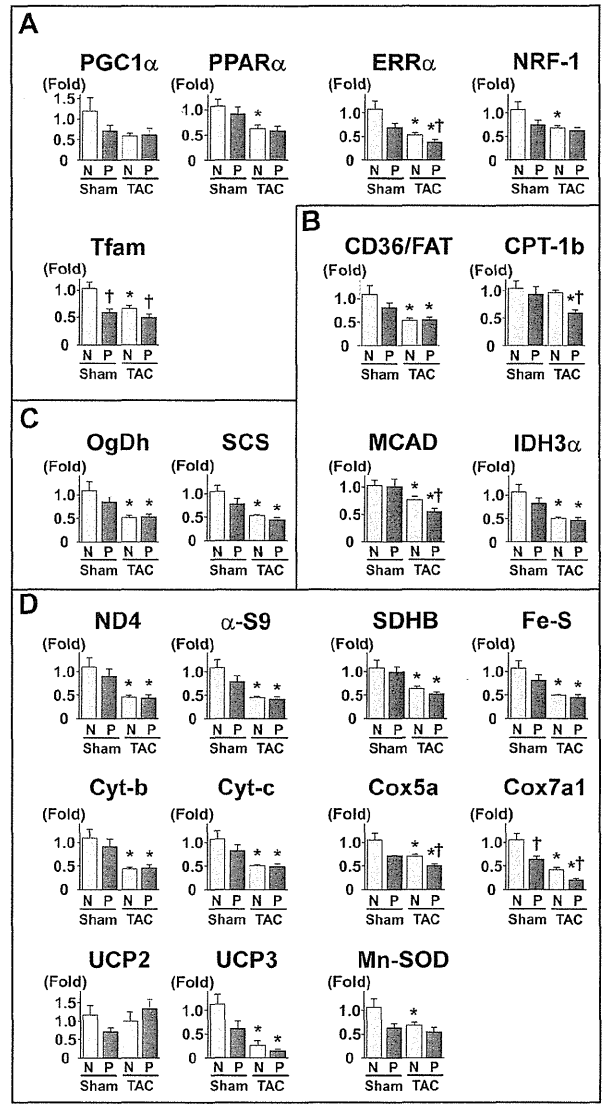

Figure 10. The expression of genes related to mitochondrial function under the TAC operation. The expression of genes related to mitochondrial energy metabolism was decreased in NTg mice with TAC. The genes presented here are (**A**) transcriptional regulators, (**B**) fatty acid metabolism, (**C**) the TCA cycle, and (**D**) mitochondria. Pgam2 overexpression further decreased the expression of some of these genes, such as ERRα, Tfam, MCAD, Cox5a, and Cox7a1 with TAC. Values are the mean ± SEM. N: NTg mice. P: Pgam2 mice. *$p<0.05$ versus the same genotype with the sham operation. †$p<0.05$ versus NTg mice with the same operation. Sham-operated NTg mice: n = 8; sham-operated Pgam2 mice: n = 8; NTg mice with TAC: n = 10; Pgam2 mice with TAC: n = 14.
doi:10.1371/journal.pone.0072173.g010

mitochondrial electron transport chain Complex II in plants [51]. GSH, aspartate, betaine, proline, and spermidine levels were decreased in Pgam2 mice.

Furthermore, the mechanism by which Pgam2 overexpression changed the gene expression of mitochondrial proteins is currently unknown. However, communication between mitochondria and the nucleus may influence many cellular activities [52], and has been referred to as "mitochondrial retrograde signaling". Signaling pathways known to be involved in this communication are the target of rapamycin (TOR) and calcium signaling. Thus, we speculate that mitochondrial retrograde signaling may be involved in the impaired gene expression of mitochondrial protein; however, further studies are required.

The effects of the persistent overexpression of Pgam2 on fatty acid metabolism are less clear because our metabolomic analysis was unable to measure lipids and fatty acids. However, it is likely that the persistent overexpression of Pgam2 modified fatty acid metabolism. The gene expression of CD36/fatty acid translocase (CD36/FAT) was normal in Pgam2 mice (Figure 6B), which was consistent with the normal uptake of ^{125}I-9MPA (Figure 2A and Table S2). However, the gene expression of CPT-1b, which is necessary for the uptake of fatty acids by mitochondria, was decreased. In addition, gene expression levels of PPARα, PPARδ, and ERRα were decreased in Pgam2 mice (Figure 6A).

The heart oxidizes the most efficient fuel for respiration in order to adapt to changes in cardiac workload, oxygen supply, and substrate availability in an appropriate manner. The normal heart exhibits such "metabolic flexibility", the loss of which is hypothesized to be involved in the development of heart failure [53]. In this study, the persistent overexpression of Pgam2 may have modified glucose, fatty acid, and mitochondrial metabolism, impaired metabolic flexibility and predispose Pgam2 mice to cardiac dysfunction under stressed conditions, such as dobutamine infusion and pressure overload.

Myocardial fibrosis was shown to be induced by several conditions, such as mechanical stress, myocardial ischemia, and inflammation [54]. It has recently become clear that energy metabolism in the cell is closely linked to inflammation [55]. For example, proinflammatory macrophages show a shift from oxidative phosphorylation to glycolysis, which mimics the metabolic change known as the Warburg effect in cancer cells. Mitochondrial dysfunction has been shown to induce inflammatory responses [56,57]. In addition, perturbations in energy metabolism predispose the heart to significant myocardial fibrosis under stressed conditions [58,59]. Thus, we suggest that a modification in energy metabolism by persistent Pgam2 overexpression may be one of the causes of the significant fibrosis observed in response to pressure overload.

Limitations of this study

We did not directly measure glycolytic flux, and, instead, estimated the flux from the results of metabolomic analysis and uptake of a glucose analog. In addition, the findings of the present study need to be interpreted with caution when we consider the role of Pgam in cardiac physiology and pathophysiology for the following reasons. First, a large amount of the Pgam protein was persistently overexpressed, which caused secondary changes that may not be related to the function of Pgam2 itself. Second, the parameters of cardiac energy metabolism, such as the phosphocreatine/βATP ratio, substrate uptake, metabolite quantification, and mitochondrial functions were not analyzed under stressed conditions. Thus, the physiological and pathophysiological roles of Pgam should be investigated in more detail in the future using the inducible overexpression of Pgam2, Pgam2 knockout mice, or inhibitors of Pgam.

Supporting Information

Figure S1 The antibody against Pgam1 also served as that against Pgam2 with a similar sensitivity. FLAG-tagged murine Pgam1 or Pgam2 was transfected into murine embryonic fibroblasts defective in p53. Total cellular lysates were analyzed by western blotting. The antibodies used were anti-Pgam1 (1:1000; Abcam, Cambridge, UK; Ab2220) and anti-FLAG (1:1000; Sigma, St. Louis, MO, USA; F1804). The similar sensitivities of the anti-Pgam1 antibody against the two isoforms of Pgam proteins were confirmed.
(TIF)

Figure S2 Mitochondrial morphology and a marker of ROS were normal in the heart tissue of Pgam2 mice. (A) Ultrastructural analysis of Pgam2 mice. Electron micrographs of histological sections of the left ventricle prepared from 12-week-old Pgam2 mice and non-transgenic littermates. The insets on the right panel are high-magnification images of the indicated portions (squares) of the images on the left. The morphology of mitochondria in Pgam2 mice was normal. Nucl.: nucleus. The bar represents 1 μm. The density (number per 100 μm^2) and the size (μm^2) of mitochondria within a cardiomyocyte were observed by electron microscopy (lower panels). Values are the mean ± SEM (n = 3 for each groups). **(B)** TBARS as a marker of oxidative stress. Thiobarbituric acid reactive substances (TBARS) levels were normal in the heart tissue of Pgam2 mice. Values are the mean ± SEM. NTg mice: n = 7; Pgam2 mice: n = 8.
(TIF)

Table S1 Primer sequences used for real-time quantitative RT-PCR.
(DOC)

Table S2 Myocardial uptake of ^{18}FDG and ^{125}I-9MPA.
(DOC)

Table S3 Concentrations of metabolites in the heart identified by metabolomic analysis.
(DOC)

Author Contributions

Conceived and designed the experiments: T. Shioi. Performed the experiments: JO SN T. Kato Y. Inuzuka T. Kawashima Y. Tamaki AK Y. Tanada Y. Iwanaga MN TM SA T. Soga GT. Analyzed the data: JO SN T. Shioi. Contributed reagents/materials/analysis tools: HK. Wrote the paper: JO SN. Supported the experiments: T. Kita T. Kimura.

References

1. Rich MW (2001) Heart failure in the 21st century: a cardiogeriatric syndrome. J Gerontol A Biol Sci Med Sci 56: M88–96.
2. Jencks SF, Williams MV, Coleman EA (2009) Rehospitalizations among patients in the Medicare fee-for-service program. N Engl J Med 360: 1418–1428.
3. Neubauer S (2007) The failing heart--an engine out of fuel. N Engl J Med 356: 1140–1151.
4. Tuunanen H, Engblom E, Naum A, Nagren K, Scheinin M, et al. (2008) Trimetazidine, a metabolic modulator, has cardiac and extracardiac benefits in idiopathic dilated cardiomyopathy. Circulation 118: 1250–1258.
5. Wallhaus TR, Taylor M, DeGrado TR, Russell DC, Stanko P, et al. (2001) Myocardial free fatty acid and glucose use after carvedilol treatment in patients with congestive heart failure. Circulation 103: 2441–2446.

6. Taylor M, Wallhaus TR, Degrado TR, Russell DC, Stanko P, et al. (2001) An evaluation of myocardial fatty acid and glucose uptake using PET with [18F]fluoro-6-thia-heptadecanoic acid and [18F]FDG in Patients with Congestive Heart Failure. J Nucl Med 42: 55–62.
7. Paolisso G, Gambardella A, Galzerano D, D'Amore A, Rubino P, et al. (1994) Total-body and myocardial substrate oxidation in congestive heart failure. Metabolism 43: 174–179.
8. Davila-Roman VG, Vedala G, Herrero P, de las Fuentes L, Rogers JG, et al. (2002) Altered myocardial fatty acid and glucose metabolism in idiopathic dilated cardiomyopathy. J Am Coll Cardiol 40: 271–277.
9. Neglia D, De Caterina A, Marraccini P, Natali A, Ciardetti M, et al. (2007) Impaired myocardial metabolic reserve and substrate selection flexibility during stress in patients with idiopathic dilated cardiomyopathy. Am J Physiol Heart Circ Physiol 293: H3270–3278.
10. Chandler MP, Kerner J, Huang H, Vazquez E, Reszko A, et al. (2004) Moderate severity heart failure does not involve a downregulation of myocardial fatty acid oxidation. Am J Physiol Heart Circ Physiol 287: H1538–1543.
11. Osorio JC, Stanley WC, Linke A, Castellari M, Diep QN, et al. (2002) Impaired myocardial fatty acid oxidation and reduced protein expression of retinoid X receptor-alpha in pacing-induced heart failure. Circulation 106: 606–612.
12. Nascimben L, Ingwall JS, Lorell BH, Pinz I, Schultz V, et al. (2004) Mechanisms for increased glycolysis in the hypertrophied rat heart. Hypertension 44: 662–667.
13. Kato T, Niizuma S, Inuzuka Y, Kawashima T, Okuda J, et al. (2010) Analysis of metabolic remodeling in compensated left ventricular hypertrophy and heart failure. Circ Heart Fail 3: 420–430.
14. Liao R, Jain M, Cui L, D'Agostino J, Aiello F, et al. (2002) Cardiac-specific overexpression of GLUT1 prevents the development of heart failure attributable to pressure overload in mice. Circulation 106: 2125–2131.
15. Zhao G, Jeoung NH, Burgess SC, Rosaaen-Stowe KA, Inagaki T, et al. (2008) Overexpression of pyruvate dehydrogenase kinase 4 in heart perturbs metabolism and exacerbates calcineurin-induced cardiomyopathy. Am J Physiol Heart Circ Physiol 294: H936–943.
16. Ashrafian H, Frenneaux MP, Opie LH (2007) Metabolic mechanisms in heart failure. Circulation 116: 434–448.
17. Zhang J, Yu L, Fu Q, Gao J, Xie Y, et al. (2001) Mouse phosphoglycerate mutase M and B isozymes: cDNA cloning, enzyme activity assay and mapping. Gene 264: 273–279.
18. Kondoh H, Lleonart ME, Gil J, Wang J, Degan P, et al. (2005) Glycolytic enzymes can modulate cellular life span. Cancer Res 65: 177–185.
19. DiMauro S, Miranda AF, Khan S, Gitlin K, Friedman R (1981) Human muscle phosphoglycerate mutase deficiency: newly discovered metabolic myopathy. Science 212: 1277–1279.
20. Chen G, Gharib TG, Wang H, Huang CC, Kuick R, et al. (2003) Protein profiles associated with survival in lung adenocarcinoma. Proc Natl Acad Sci U S A 100: 13537–13542.
21. Hitosugi T, Zhou L, Elf S, Fan J, Kang HB, et al. (2012) Phosphoglycerate mutase 1 coordinates glycolysis and biosynthesis to promote tumor growth. Cancer Cell 22: 585–600.
22. Evans MJ, Saghatelian A, Sorensen EJ, Cravatt BF (2005) Target discovery in small-molecule cell-based screens by in situ proteome reactivity profiling. Nat Biotechnol 23: 1303–1307.
23. Durany N, Carreras J (1996) Distribution of phosphoglycerate mutase isozymes in rat, rabbit and human tissues. Comp Biochem Physiol B Biochem Mol Biol 114: 217–223.
24. Heinke MY, Wheeler CH, Yan JX, Amin V, Chang D, et al. (1999) Changes in myocardial protein expression in pacing-induced canine heart failure. Electrophoresis 20: 2086–2093.
25. Subramaniam A, Jones WK, Gulick J, Wert S, Neumann J, et al. (1991) Tissue-specific regulation of the alpha-myosin heavy chain gene promoter in transgenic mice. J Biol Chem 266: 24613–24620.
26. Ng WA, Grupp IL, Subramaniam A, Robbins J (1991) Cardiac myosin heavy chain mRNA expression and myocardial function in the mouse heart. Circ Res 68: 1742–1750.
27. Shioi T, Kang PM, Douglas PS, Hampe J, Yballe CM, et al. (2000) The conserved phosphoinositide 3-kinase pathway determines heart size in mice. EMBO J 19: 2537–2548.
28. Inuzuka Y, Okuda J, Kawashima T, Kato T, Niizuma S, et al. (2009) Suppression of phosphoinositide 3-kinase prevents cardiac aging in mice. Circulation 120: 1695–1703.
29. Bottomley PA (1985) Noninvasive study of high-energy phosphate metabolism in human heart by depth-resolved 31P NMR spectroscopy. Science 229: 769–772.
30. Soga T, Ohashi Y, Ueno Y, Naraoka H, Tomita M, et al. (2003) Quantitative metabolome analysis using capillary electrophoresis mass spectrometry. J Proteome Res 2: 488–494.
31. Palmer JW, Tandler B, Hoppel CL (1977) Biochemical properties of subsarcolemmal and interfibrillar mitochondria isolated from rat cardiac muscle. J Biol Chem 252: 8731–8739.
32. Kawashima T, Inuzuka Y, Okuda J, Kato T, Niizuma S, et al. (2011) Constitutive SIRT1 overexpression impairs mitochondria and reduces cardiac function in mice. J Mol Cell Cardiol 51: 1026–1036.
33. Nakagawa M, Takemura G, Kanamori H, Goto K, Maruyama R, et al. (2008) Mechanisms by which late coronary reperfusion mitigates postinfarction cardiac remodeling. Circ Res 103: 98–106.
34. Date MO, Morita T, Yamashita N, Nishida K, Yamaguchi O, et al. (2002) The antioxidant N-2-mercaptopropionyl glycine attenuates left ventricular hypertrophy in in vivo murine pressure-overload model. J Am Coll Cardiol 39: 907–912.
35. Neubauer S, Horn M, Cramer M, Harre K, Newell JB, et al. (1997) Myocardial phosphocreatine-to-ATP ratio is a predictor of mortality in patients with dilated cardiomyopathy. Circulation 96: 2190–2196.
36. Chacko VP, Aresta F, Chacko SM, Weiss RG (2000) MRI/MRS assessment of in vivo murine cardiac metabolism, morphology, and function at physiological heart rates. Am J Physiol Heart Circ Physiol 279: H2218–2224.
37. Iyer NV, Kotch LE, Agani F, Leung SW, Laughner E, et al. (1998) Cellular and developmental control of O2 homeostasis by hypoxia-inducible factor 1 alpha. Genes Dev 12: 149–162.
38. Kelly GJ, Turner JF (1970) The regulation of pea-seed phosphofructokinase by 6-phosphogluconate, 3-phosphoglycerate, 2-phosphoglycerate and phosphoenolpyruvate. Biochim Biophys Acta 208: 360–367.
39. Hayashi D, Ohshima S, Isobe S, Cheng XW, Unno K, et al. (2013) Increased (99m)Tc-sestamibi washout reflects impaired myocardial contractile and relaxation reserve during dobutamine stress due to mitochondrial dysfunction in dilated cardiomyopathy patients. J Am Coll Cardiol 61: 2007–2017.
40. Sheridan DJ, Autelitano DJ, Wang B, Percy E, Woodcock EA, et al. (2000) Beta(2)-adrenergic receptor overexpression driven by alpha-MHC promoter is downregulated in hypertrophied and failing myocardium. Cardiovasc Res 47: 133–141.
41. Brand MD, Nicholls DG (2011) Assessing mitochondrial dysfunction in cells. Biochem J 435: 297–312.
42. Perry CG, Kane DA, Lanza IR, Neufer PD (2013) Methods for assessing mitochondrial function in diabetes. Diabetes 62: 1041–1053.
43. O'Neill BT, Kim J, Wende AR, Theobald HA, Tuinei J, et al. (2007) A conserved role for phosphatidylinositol 3-kinase but not Akt signaling in mitochondrial adaptations that accompany physiological cardiac hypertrophy. Cell Metab 6: 294–306.
44. Kondoh H, Lleonart ME, Nakashima Y, Yokode M, Tanaka M, et al. (2007) A high glycolytic flux supports the proliferative potential of murine embryonic stem cells. Antioxid Redox Signal 9: 293–299.
45. Nathan Baily C, Cason RW, Vadvalkar SS, Matsuzaki S, Humphries KM (2011) Inhibition of mitochondrial respiration by phosphoenolpyruvate. Arch Biochem Biophys 514: 68–74.
46. Drose S (2013) Differential effects of complex II on mitochondrial ROS production and their relation to cardioprotective pre- and postconditioning. Biochim Biophys Acta 1827: 578–587.
47. Wullner U, Seyfried J, Groscurth P, Beinroth S, Winter S, et al. (1999) Glutathione depletion and neuronal cell death: the role of reactive oxygen intermediates and mitochondrial function. Brain Res 826: 53–62.
48. Heales SJ, Davies SE, Bates TE, Clark JB (1995) Depletion of brain glutathione is accompanied by impaired mitochondrial function and decreased N-acetyl aspartate concentration. Neurochem Res 20: 31–38.
49. Sivakumar R, Anandh Babu PV, Shyamaladevi CS (2008) Protective effect of aspartate and glutamate on cardiac mitochondrial function during myocardial infarction in experimental rats. Chem Biol Interact 176: 227–233.
50. Ganesan B, Rajesh R, Anandan R, Dhandapani N (2007) Biochemical studies on the protective effect of betaine on mitochondrial function in experimentally induced myocardial infarction in rats. Journal of Health Science 53: 671–681.
51. Hamilton EW, (2001) Mitochondrial adaptations to NaCl. Complex I is protected by anti-oxidants and small heat shock proteins, whereas complex II is protected by proline and betaine. Plant Physiol 126: 1266–1274.
52. Butow RA, Avadhani NG (2004) Mitochondrial signaling: the retrograde response. Mol Cell 14: 1–15.
53. Taegtmeyer H, Golfman L, Sharma S, Razeghi P, van Arsdall M (2004) Linking gene expression to function: metabolic flexibility in the normal and diseased heart. Ann N Y Acad Sci 1015: 202–213.
54. Swynghedauw B (1999) Molecular mechanisms of myocardial remodeling. Physiol Rev 79: 215–262.
55. O'Neill LA, Hardie DG (2013) Metabolism of inflammation limited by AMPK and pseudo-starvation. Nature 493: 346–355.
56. Aguilera-Aguirre L, Bacsi A, Saavedra-Molina A, Kurosky A, Sur S, et al. (2009) Mitochondrial dysfunction increases allergic airway inflammation. J Immunol 183: 5379–5387.
57. Basu Ball W, Kar S, Mukherjee M, Chande AG, Mukhopadhyaya R, et al. (2011) Uncoupling protein 2 negatively regulates mitochondrial reactive oxygen species generation and induces phosphatase-mediated anti-inflammatory response in experimental visceral leishmaniasis. J Immunol 187: 1322–1332.
58. Wang J, Xu J, Wang Q, Brainard RE, Watson LJ, et al. (2013) Reduced cardiac fructose 2,6 bisphosphate increases hypertrophy and decreases glycolysis following aortic constriction. PLoS One 8: e53951.
59. Watanabe K, Fujii H, Takahashi T, Kodama M, Aizawa Y, et al. (2000) Constitutive regulation of cardiac fatty acid metabolism through peroxisome proliferator-activated receptor alpha associated with age-dependent cardiac toxicity. J Biol Chem 275: 22293–22299.

臓器移植法改正後の心臓移植

中谷武嗣[1)]　築瀬正伸[2)]　藤田知之[2)]
1) 国立循環器病研究センター移植部，2) 同　心臓外科

はじめに

わが国においては，1997年10月に臓器の移植に関する法律が施行され，この法律に基づく心臓移植が1999年2月に行われ，引き続き同年5月，6月にも行われた[1)2)]．なお，最初の2例はともに補助人工心臓(ventricular assist system；VAS)によるブリッジ例であった．その後，施行数は年間数例であったが，徐々に増加し，2006年には年間施行数が10例となった(**図1**)．しかし，心臓移植希望者数も増加したため，待機期間は長期化し，成人例における心臓移植実施例は全例status 1で，その9割は補助人工心臓によるブリッジ例であった．脳死下での臓器提供数を増やすための検討がなされ，遺族同意により脳死者からの臓器提供を可能とする改正臓器移植法が2009年に制定され，2010年7月から施行された．この結果，改正臓器移植法が施行される2010年6月までの11年間における心臓移植実施数69例に対し，臓器移植法改正後2012年12月までの2年6カ月の施行数は79例と著明に増加し，年間30例程度の状況となり，さらに，10歳未満の小児からの提供による心臓移植も1例行われた(**図1**)．また，2011年4月からは，植込型非拍動流補助人工心臓の心臓移植へのブリッジ使用が保険償還されるようになった．このため，わが国における心臓移植の状況は大きく変わりつつあり，本稿において現状と今後の展望について述べる．

わが国における現状

2012年の本邦心臓移植登録報告によると[3)]，日本臓器移植ネットワークへの心臓移植希望登録は2012年10月31日時点で624名あり，わが国で144名の心臓移植と1例の心肺移植が実施され，42名は海外渡航移植を行い，235名(うち4例は心肺移植希望)が待機中である．なお，待機中の63%はstatus 1であった．

2012年11月25日までにわが国においては146例の心臓移植が施行された．わが国における心臓移植実施施設は現在9施設で，その施行数は，国立循環器病研究センター：52例，大阪大学：42例，東京大学：

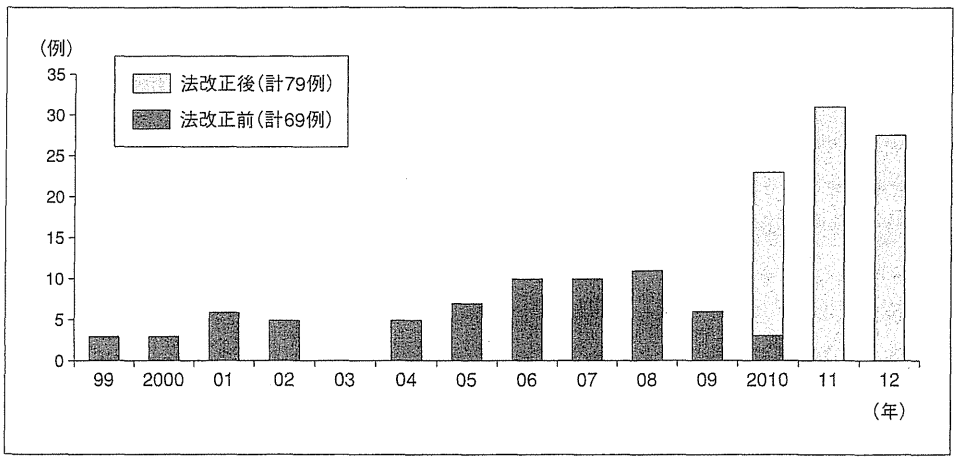

図1
わが国における心臓移植の推移

26例，東京女子医科大学：10例，九州大学：6例，東北大学：5例，埼玉医科大学(国際医療センター)5例であった．

心臓移植施行例の年齢は平均37.5歳で，原因疾患は，特発性拡張型心筋症が68%と最も多く，虚血性心筋症は10%であった．待機状況は，10歳未満の1例がstatus 2であった以外はstatus 1であった．また，そのうち89%は補助人工心臓によるブリッジ例であった．Status 1での待機期間は平均854日で，待機1年以内での施行例は8%であった．また，補助人工心臓ブリッジ例の補助期間は平均876日であった．

移植後10年の生存率は91.6%と国際心肺移植学会レジストリーでの成績より良好である(**図2**)[3)4)]．死亡は8例で，その死因は多臓器不全2例，感染症3例，移植後冠動脈病変，胃癌，腎不全がそれぞれ1例であった．

国立循環器病研究センターにおける現状

2012年12月31日までに52例の心臓移植を施行したが，移植時年齢は平均37歳で，補助人工心臓装着中の60歳以上症例が3例含まれている[5)]．待機状況は全例status 1で，90%は各種左心補助装置(left ventricular assist system；LVAS)によるブリッジ例で，用いたLVASは，87%が体外設置型(Nipro製国循型)であった．また，status 1での待機期間は平均838日で最長は1,476日に及んだ．また，LVAS補助期間は平均886日で，最長は体外設置型による1703日であった．これまで2例が感染症で死亡したが，10年生存率は93.9%で，2例が13年以上経過し，元気に過ごしている．また，ドナーでは，79%がマージナルであり，移植後9例においてprimary graft dysfunctionを認め，IABPやPCPSによる補助を4例に行ったが全例離脱し，移植後早期死亡はなく4週後において心エコー上，有意な差を認めなかった[6)]．

現在生存中の50例において，入院加療中およびリハビリ中が23%であるが，ほかは，復職，再就職，復学，主婦などの社会復帰を行っている．

なお，法改正前の12年間に27例を施行し，法改正後の2年半で25例を実施したが，status 1での待機日数およびLVASによる補助期間は，それぞれ平均750日から947日へ，および762日から1,028日へと著明に増加していた(**図3**)．

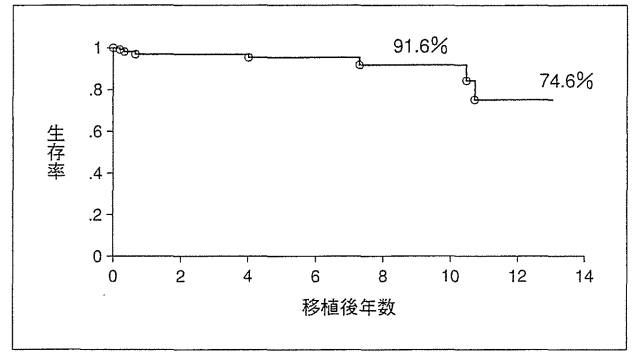

図2　わが国における心臓移植の生存率
(文献3より改変引用)

臓器移植法改正後の課題

1．移植希望者数の増加

わが国における心臓移植の適応判定は，施設における検討会に加え，日本循環器学会心臓移植適応検討小委員会(以下小委員会)での適応検討が必要であり，この内科系および外科系委員を含む小委員会での適応判定が日本臓器移植ネットワークへの心臓移植希望登録に必須である．これまでの小委員会への年間新規申請数は，臓器移植法が制定された1997年から2007年までは40例/年前後であった．2006年にはわが国での心臓移植実施数が年間10例となり，施行例の成績も良好であることが徐々に認知されるようになり，希望者数も増加した．このため，2008～2010年までの小委員会への新規申請数は年間70例を超えるまでに増加した．さらに，臓器移植法が改正され，年間施行数が30例前後となった2011年からの2年間では年間100例を超えるようになった．小委員会では，委員数を増やすとともにグループ分けを行うことで対応されてきた．しかし，2012年には再申請分を含めると2～3例/週の申請がある状況となり，小委員会での対応が困難となってきている．そこで，心臓移植実施施設で協議体を構築し，移植施設からの申

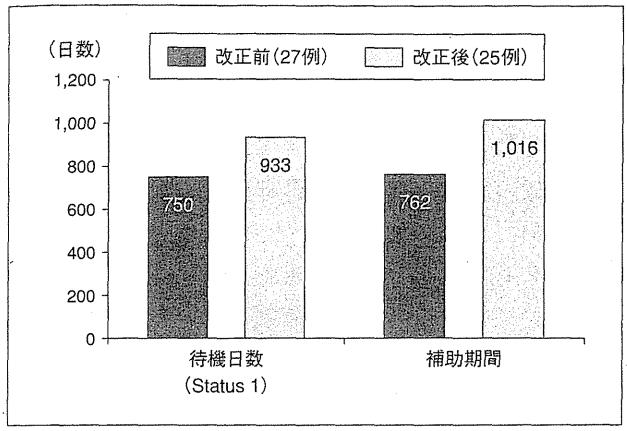

図3　国立循環器病研究センターにおける心臓移植待機日数および補助期間

請に関してはこの心臓移植実施施設協議体で行うことが検討された．しかし，現状では実施施設では申請作業も行っており，対応が困難であるとされた．その後，移植実施数の増加に伴い，各施設での経験数が増加し，2012年後半には経験数が50例を超える施設が出てきた．そこで，心臓移植経験数が50例を超えた施設では，自施設での検討による移植適応判定により日本臓器移植ネットワークへの登録申請が行えるようにし，小委員会へは同時に報告を行うこととし，これらの症例に関しては日本循環器学会心臓移植委員会で検証を行う体制を構築することで対応する検討が進められている．わが国での2段階での適応検討制度を変更するには，心臓移植関連学会協議会，さらには移植関係学会合同委員会での検討も必要であり，その作業も開始されている．

2. 小児心臓移植

臓器移植法の改正により，小児例における脳死臓器提供が行えるようになった．その実施に当たって，小児からの提供に対し，小児での移植希望者に優先的に配分されることが要望され，厚生労働省の心臓移植の基準に関する作業班において検討がなされた．その結果，ドナーが18歳未満の場合には，18歳未満(登録時)の移植希望者を優先することとなった．これまでに，18歳未満からの提供により，3例の心臓移植が行われており，うち1例は10歳未満からの提供であった．

小児心臓移植における問題として，小児用の補助人工心臓がわが国にないことがある．わが国での心臓移植の成人例では，待機期間が長いため，補助人工心臓によるブリッジ例が大部分を占めており，小児例に用いることができる小児用補助人工心臓が望まれる．欧米では，ドイツで開発されたExcor小児用体外設置型補助人工心臓が用いられている．現在わが国においても，Excor小児用体外設置型補助人工心臓の医師主導での臨床治験が進められており，早期の保険収載が望まれている．

3. 心臓移植適応年齢の拡大

1997年の臓器移植法制定時においては，脳死ドナー不足が当初から想定されており，また，当時の社会状況では定年がおおむね60歳までであったこともあり，心臓移植適応における年齢においては，60歳未満が望ましいとされた．その後，社会情勢も大きく変わり，また，医療の進歩に伴い高齢者に対しても手術を含む治療が積極的に行われるようになり，その治療成績も向上してきた．このような状況において，60歳以上の症例での心不全例に対しても心臓移植が考慮されるべきとされるようになった．そこで，日本循環器学会心臓移植委員会で検討が行われ，ドナー臓器の配分へも配慮した提案がなされた．この提案について厚生労働省の心臓移植の基準に関する作業班で検討された．そこで，ドナー配分に60歳未満での申請例と60歳以上での申請例を分けたシステムで開始することで，年齢条項が65歳未満が望ましいに引き上げられ，2013年2月から日本臓器移植ネットワークでの登録が開始された．これまで，LVAS装着にて60歳以上で移植された症例もあり，今回の改正による60歳以上での移植例も含め，その成績を検討し，ドナー配分については再度検討することとなっている．

4. 高齢などマージナルドナー増加とその対策

臓器移植法の改正により家族の同意による提供が可能となったが，60歳を超える症例においても，心

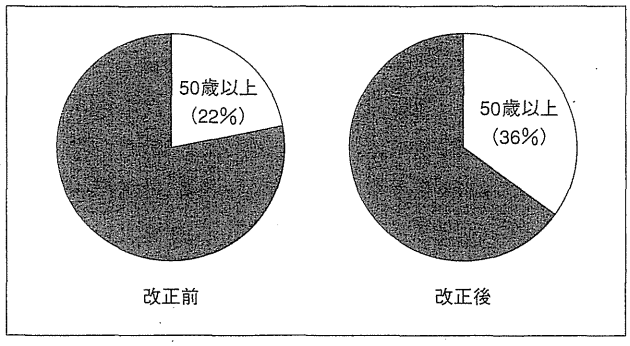

図4　国立循環器病研究センターにおけるドナーの年齢

臓提供の希望が呈示されることが多くなった．当センターにおいても，改正後レシピエントの平均年齢は39歳から34歳となったが，提供者における50歳以上の占める割合が著明に増加している(図4)．高齢者においては，心疾患を伴う可能性が高く，冠動脈の病変に対する評価ができる体制とすることが今後の課題である．また，メディカルコンサルタント制度の導入により，わが国におけるドナーの利用率は非常に高い．しかし，メディカルコンサルタントが介入できる時期が1回目の脳死判定が終了してからであるため，時間的制約がある．また，移植希望者の状況に応じたドナーの選択が必要であるが，移植施設への連絡が2回の脳死判定終了後となるため，対応に苦慮しているのが現状である．

5. 植込型補助人工心臓

わが国では長期の心臓待機を必要とするため，補助人工心臓によるブリッジ例が大部分を占めており，在宅治療可能な植込型LVASが長く望まれてきた．2011年4月になり，わが国で開発された2種の非拍動流型植込型LVASが心臓移植へのブリッジとして保険償還された．また，植込型補助人工心臓実施施設および実施医の認定も補助人工心臓関連学会協議会においてなされるようになり，さらに，4学会1研究会による人工心臓管理技術認定士制度の整備も進んでいる．これらにより，従来の拍動流型植込型補助人工心臓施行施設が心臓移植施設に限られていたのに対し，植込型非拍動流型補助人工心臓施行は，認定された移植施設以外の実施施設でも行えるようになった．また，在宅での管理に関しても健康保険での指導管理料が設置されるようになり，植込型補助人工心臓装着を行う施設も増えつつある．さらに，心臓移植の年齢条項が65歳未満となったことより，ブリッジ例としての使用が増加すると見込まれる．心臓移植の代替治療としての植込型補助人工心臓の適応について検討を進める段階にきている．

おわりに

末期心不全に対して，わが国においても心臓移植および補助人工心臓が治療選択として受け入れられるようになり，その施行数も増加し，その成績は良好である．臓器移植法の改正により，施行数の増加とともに小児での心臓移植が施行できるようになった．さらに，心臓移植の適応年齢が，60歳未満が望ましいから65歳未満が望ましいに変更された．また，植込み型補助人工心臓が心臓移植へのブリッジとして保険償還され，さらに，心臓移植施設以外でも植込み型補助人工心臓の使用が行える体制となっている．

今後，わが国での末期心不全に対する心臓移植，および補助人工心臓を組み入れた治療体系の整備を進める必要である．

文　献

1) Nakatani T : Heart transplantation. *Circ J* 2009 ; **73**(Suppl A) : A55-60
2) 中谷武嗣，藤田知之：臓器移植の新時代 わが国における脳死移植の現状と今後　心臓移植．医学のあゆみ 2011 ; **237** : 397-403
3) 日本心臓移植研究会．本邦心臓移植登録報告(2012年)．移植 2012 ; **47** : 429-432
4) Stehlik J, Edwards LB, Kucheryavaya AY, et al : The registry of the International Society for Heart and Lung Transplantation : 29th official adult heart transplant report--2012. *J Heart Lung Transplant* 2012 ; **31** : 1052-1064
5) 中谷武嗣，秦　広樹，藤田知之，ほか：重症心不全に対する外科治療 心臓移植および補助人工心臓の経験．胸部外科 2013 ; **66** : 63-67
6) Fujita T, Toda K, Yanase M, et al : Risk factors for post-transplant low output syndrome. *Eur J Cardiothorac Surg* 2012 ; **42** : 551-556

Heart Vessels
DOI 10.1007/s00380-013-0452-9

ORIGINAL ARTICLE

Evaluation of coronary artery disease and cardiac morphology and function in patients with hypertrophic cardiomyopathy, using cardiac computed tomography

Satoshi Okayama · Tsunenari Soeda · Rika Kawakami · Yasuhiro Takami · Satoshi Somekawa · Tomoya Ueda · Yu Sugawara · Takaki Matsumoto · Ji Hee Sung · Taku Nishida · Shiro Uemura · Yoshihiko Saito

Received: 2 July 2013 / Accepted: 29 November 2013

Abstract Coronary artery disease and cardiac morphology and function were evaluated in 51 patients with hypertrophic cardiomyopathy (HCM), without typical chest pain, using cardiac computed tomography (CT). This study investigated the prevalence of coronary artery disease, the indicators of obstructive coronary stenosis, and the magnitude of left ventricular (LV) hypertrophy. The patients' mean coronary artery calcium score was 198.8 ± 312.0 and was positively correlated with the number of coronary risk factors ($r = 0.32$; $P < 0.05$). Of the 51 patients with HCM, 42 (82.4 %) had some degree of stenosis and 8 (15.7 %) had obstructive stenosis. Noncalcified and mixed plaques were detected in 14 (27.5 %) and 11 (21.6 %) patients, respectively. Multivariate logistic regression revealed that diabetes was an independent indicator of the presence of obstructive stenosis in HCM patients. Multivariate linear regression revealed that low estimated glomerular filtration rates and high triglyceride concentrations were independent indicators of higher LV mass indexes. In conclusion, cardiac CT revealed that coronary artery disease was common among patients with HCM. The presence of obstructive coronary stenosis and the magnitude of LV hypertrophy were related to the presence of diabetes, triglyceride levels, and estimated glomerular filtration rate.

S. Okayama (✉) · T. Soeda · R. Kawakami · Y. Takami · S. Somekawa · T. Ueda · Y. Sugawara · T. Matsumoto · T. Nishida · S. Uemura · Y. Saito
First Department of Internal Medicine, Nara Medical University, 840 Shijo-cho, Kashihara, Nara 634-8522, Japan
e-mail: satosi01@naramed-u.ac.jp

J. H. Sung
Department of Cardiology, Yamato-Kashihara Hospital, Nara, Japan

Keywords Hypertrophic cardiomyopathy · Coronary artery disease · Computed tomography · Diabetes

Introduction

Hypertrophic cardiomyopathy (HCM) is a common genetic cardiac disease with a prevalence of 0.2 %, characterized by a small left ventricular (LV) cavity and regional myocardial hypertrophy [1]. Many HCM patients remain stable throughout their lives; however, a small but significant minority experience sudden cardiac death, heart failure, or atrial fibrillation [2–5]. Coronary artery disease is an important cause of sudden cardiac death and heart failure, and reportedly has adverse effects on the prognosis of patients with HCM [6]; however, its prevalence and risk factors have not been sufficiently evaluated in patients with HCM.

Cardiac computed tomography (CT) permits a minimally invasive evaluation of coronary artery stenosis and plaques [7–9] as well as the morphology and function of the left ventricle and left atrium [10, 11]. Cardiac CT has also been reported to be useful for the evaluation of myocardial fibrosis in patients with HCM [12, 13]; however, there have only been a few reports on the evaluation of coronary artery anatomy and cardiac morphology and function [13–17]. We believe that the evaluation of coronary plaques by cardiac CT may be useful for managing patients with HCM because the presence of coronary artery disease, detected by catheter-based angiography, is associated with a worse prognosis in patients with HCM [6]. The purposes of this study were: (1) to investigate the prevalence of coronary artery disease, and (2) to determine the indicators of obstructive coronary stenosis and the magnitude of LV hypertrophy in patients with HCM, using cardiac CT.

Published online: 11 December 2013

Patients and methods

Patients

Between April 1, 2010 and August 31, 2012, 61 consecutive HCM patients underwent cardiac CT at Nara Medical University and Yamato-Kashihara Hospital and were enrolled in this study. The exclusion criteria were as follows: (1) history of myocardial infarction; (2) percutaneous transluminal septal myocardial ablation, coronary intervention, or coronary artery bypass grafting; (3) typical chest pain defined as pressure-like retrosternal pain exacerbated by exercise and relieved at rest or by administration of nitroglycerin [18]; (4) structural heart disease, as evidenced by previous echocardiography; (5) secondary cardiomyopathy, such as Fabry disease, amyloidosis, and mitochondrial cardiomyopathy, which presents as an HCM-like disease complicated by diabetes [19]; and (6) poor image quality and insufficient clinical data. Consequently, 10 patients were excluded from the analyses, allowing the retrospective analysis of 51 HCM patients. The present study was performed under clinical research protocols in accordance with the Helsinki Declaration of 1975.

HCM was diagnosed by the presence of LV hypertrophy (wall thickness of >15 mm) on cardiac CT images, in the absence of other cardiac or systemic diseases that could have resulted in the hypertrophy [1]. LV outflow obstruction was defined as a peak intraventricular pressure gradient of >30 mmHg by continuous-wave Doppler echocardiography under resting conditions [20].

The following cardiovascular risk factors were evaluated in each patient: age, gender, presence of hypertension, dyslipidemia, diabetes mellitus, and current smoking habits [21]. Advanced age was defined as >45 years for men and >55 years for women. Diabetes was defined as a nonfasting blood glucose level of >200 mg/dl, a fasting blood glucose level of ≥126 mg/dl, or current treatment with hypoglycemic agents. Dyslipidemia was defined as a low-density lipoprotein (LDL)-cholesterol level of >140 mg/dl, a high-density lipoprotein (HDL)-cholesterol level of <40 mg/dl, a triglyceride level of >150 mg/dl, or the current use of a statin or fibrate. Hypertension was defined as systolic blood pressure (BP) of ≥140 mmHg, diastolic BP ≥90 mmHg, or the current use of an antihypertensive drug for the treatment of blood pressure elevation. Patients were defined as current smokers if they had smoked regularly within the past 12 months. The estimated glomerular filtration rate was calculated by the modified formula proposed by the Japanese Society of Nephrology [22].

Cardiac computed tomography

Cardiac CT was performed using a 128-slice dual-source scanner (Somatom Definition Flash; Siemens Medical Solutions, Forchheim, Germany) at the Nara Medical University or using a 128-slice single-source scanner (Somatom Definition AS+; Siemens Medical Solutions) at the Yamato-Kashihara Hospital. β-Blockers were administered to patients with heart rates of >75 beats/min at the Yamato-Kashihara Hospital, but not at the Nara Medical University; nitrates were administered before the CT examination at both sites.

First, the coronary artery calcium score was measured, and noncontrast images were obtained with prospective electrocardiographic (ECG) gating. Next, for coronary angiography, a nonionic contrast medium, iopamidol (50–70 ml; 370 mg I/ml; Iopamiron 370; Bayer-Schering Pharma, Leverkusen, Germany), was injected at a rate of 4.0 ml/s through the right antecubital vein, followed by the injection of 40 ml of a 50:50 mixture of saline and contrast medium, at the same rate. The scan was performed using retrospective ECG gating and the bolus tracking method; images were obtained in a craniocaudal direction during a single inspiratory breath-hold.

Cardiac CT data sets were reconstructed at a 0.75-mm slice thickness and 0.4-mm slice increments, during the phase with the fewest motion artifacts, to evaluate the coronary artery, and at a 1.0-mm slice thickness and 1.0-mm slice increments at 10 % intervals throughout the cardiac cycle for the evaluation of cardiac morphology and function.

Two experienced cardiologists, blinded to the patient's background information, analyzed each patient's cardiac CT images using a three-dimensional image analysis workstation (TeraRecon Aquarius Workstation; TeraRecon, San Mateo, CA, USA). The coronary artery calcium score was calculated using the Agatston method [23]. Next, all interpretable coronary segments were evaluated for the presence of atherosclerotic plaque, using the 17-segment model of the American Heart Association [24]. Plaques were classified as noncalcified plaques, calcified plaques, and mixed plaques, as described previously [25, 26]. The noncalcified component of a plaque was defined as a lesion with a CT value higher than that of the neighboring soft tissue and a CT value lower than that of the luminal contrast. A calcified component was defined as a lesion with a CT value higher than that of the luminal contrast. A plaque containing a calcified component representing <25 % of its volume was visually categorized as a noncalcified plaque; 25–75 % as mixed plaque; and >75 % as calcified plaque. In segments containing more than one plaque, the characteristics of the most stenotic plaque were recorded. For

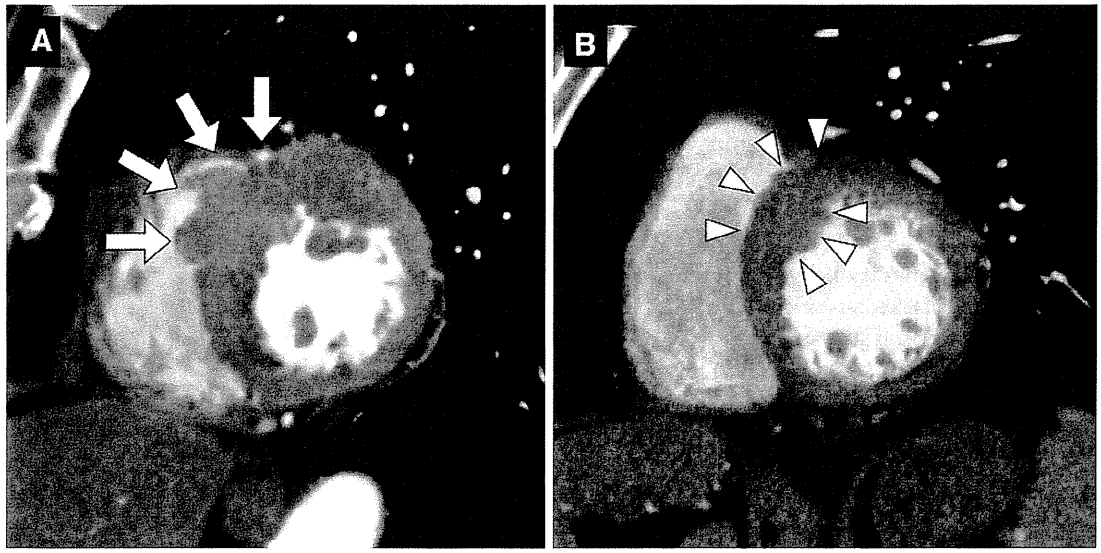

Fig. 1 Representative cases of hypertrophic cardiomyopathy with hypertrophied right ventricular trabeculation in the interventricular septum (**a**, *arrows*) and with abnormal regional left ventricular bulging (**b**, *arrowheads*)

each patient, the segment number containing each type of coronary plaque was determined. Coronary artery stenoses were visually classified as none (without any plaque), nonobstructive (<50 % luminal narrowing), or obstructive (>50 % luminal narrowing).

Cardiac morphology and function were evaluated only in patients with normal sinus rhythm. The end-diastolic and systolic phases were visually determined by the cinematic display. Septal wall thickness and septum-to-lateral wall thickness ratios were measured at the end-diastolic phase. The location of maximal LV wall thickness, hypertrophied right ventricular trabeculation in the interventricular septum (Fig. 1a, arrows), and abnormal regional LV bulging (Fig. 1b, arrowheads) were evaluated according to the report by Sipola et al. [27]. Next, multiplanar reformations in the short-axis orientation (thickness, 1.0 mm; interslice gap, 10 mm) were calculated from the axial images. LV endocardial and epicardial contours at end-diastole and systole, as well as left atrial (LA) endocardial contours at end-systole, were manually traced, as previously described [10, 11]. Pulmonary veins and LA appendages were excluded from the left atrium at their ostia. The following parameters were calculated using the modified Sympson rule: left ventricular end-diastolic volume (LVEDV), LVEDV index, myocardial volume, LV end-systolic volume (LVESV), LVESV index, LV ejection fraction (LVEF), maximum LA volume obtained at end-systole (LAV), and LAV index. LV mass was calculated by multiplying the myocardial volume by the myocardial specific gravity (1.05 g/cm^3). The magnitude of the LV hypertrophy was evaluated by calculating the LV mass index.

Statistics

We used JMP (SAS Institute, Cary, NC, USA) to analyze the data. Data are presented as mean ± standard deviation. The Chi-square test or Fisher's exact test was used for the analysis of univariate associations between categorical variables, and the Mann–Whitney U test was used for continuous variables. Indicators of the presence of obstructive coronary stenosis were determined using multivariate logistic regression analysis of clinical characteristics with a P value less than 0.1 in the univariate analysis, and indicators of LV mass index were determined using multivariate linear regression analysis. $P < 0.05$ was considered statistically significant.

Results

The study subjects consisted of 51 HCM patients (31 men and 20 women; mean age 68.6 ± 11.8 years), whose characteristics are shown in Table 1. Hypertension, dyslipidemia, diabetes, and current smoking were observed in 16 (31.4 %), 28 (54.9 %), 8 (15.7 %), and 4 (7.8 %) patients, respectively. The average number of traditional coronary risk factors in each patient was 2.7 ± 1.1. Based on the medical history, we noted that a family history of HCM and coronary artery disease was present in 3 (5.8 %) patients each. The estimated glomerular filtration rate was slightly low (62.6 ± 20.6 ml/min/1.73 m^2), and the level of plasma B-type natriuretic peptide was high (197.6 ± 250.2 pg/ml).

Table 1 Clinical characteristics of patients with hypertrophic cardiomyopathy

	Total (N = 51)	With obstructive stenosis (n = 8)	Without obstructive stenosis (n = 43)	P value
Age (years)	68.6 ± 11.8	70.6 ± 9.6	68.2 ± 12.3	0.96
Men	31 (60.8)	7 (87.5)	24 (55.8)	0.13
Body mass index (kg/m^2)	24.3 ± 3.4	23.4 ± 4.7	23.4 ± 4.7	0.49
Hypertension	16 (31.4)	3 (37.5)	13 (30.2)	0.69
Dyslipidemia	28 (54.9)	4 (50.0)	25 (58.1)	0.71
Diabetes mellitus	8 (15.7)	4 (50.0)	4 (9.3)	<0.05
Current smoking habits	4 (7.8)	2 (25.0)	2 (4.7)	0.12
No. of coronary risk factors	2.7 ± 1.1	3.4 ± 0.9	2.5 ± 1.1	<0.05
Laboratory findings				
Fasting blood glucose (mg/dl)	110.6 ± 26.3	117.9 ± 23.2	109.4 ± 26.9	0.3
HbA1c (%)	6.0 ± 0.5	6.3 ± 0.5	5.9 ± 0.4	0.06
Triglycerides (mg/dl)	138.8 ± 60.5	139.3 ± 51.6	136.6 ± 60.9	0.65
Total cholesterol (mg/dl)	196.3 ± 34.0	199.0 ± 28.5	195.2 ± 34.6	0.68
LDL-C (mg/dl)	114.4 ± 29.1	113.6 ± 23.5	114.6 ± 30.4	0.91
HDL-C (mg/dl)	53.4 ± 12.7	53.4 ± 13.4	53.4 ± 12.6	0.97
Serum creatinine (mg/dl)	0.9 ± 0.2	0.9 ± 0.2	0.9 ± 0.2	0.81
eGFR (ml/min/1.73^2)	62.6 ± 20.6	64.3 ± 12.0	62.6 ± 22.0	0.49
BNP (pg/ml)	197.6 ± 250.2	131.2 ± 77.3	210.9 ± 270.7	0.69
Medical therapy				
Oral antidiabetic agents	7 (13.7)	3 (37.5)	4 (9.3)	0.07
ACE inhibitor	9 (17.6)	1 (12.5)	8 (18.6)	1
ARB	30 (58.8)	5 (62.5)	25 (58.1)	1
β-Blocker	27 (52.9)	1 (12.5)	26 (60.5)	<0.05
Calcium antagonist	18 (35.3)	2 (25.0)	16 (37.2)	0.7
Statins	13 (25.5)	2 (25.0)	11 (25.6)	1

Values are mean ± standard deviation or number (%) of patients

HbA1c hemoglobin A1c, *LDL-C* low-density lipoprotein cholesterol, *HDL-C* high-density lipoprotein cholesterol, *eGFR* estimated glomerular filtration rate, *BNP* B-type natriuretic peptide, *ACE* angiotensin-converting enzyme, *ARB* angiotensin receptor blocker

Cardiac CT provided evaluable coronary angiography images for all subjects, and the coronary artery disease analysis is summarized in Table 2. The mean coronary artery calcium score was 198.8 ± 312.0 and was positively correlated with a number of coronary risk factors ($r = 0.32$, $P < 0.05$). Coronary stenosis was not observed in 9 (17.6 %) patients, whereas some degree of stenosis was detected in 42 (82.4 %) patients, including 34 (66.7 %) with non-obstructive stenosis and 8 (15.7 %) with obstructive stenosis. Among the patients with obstructive stenosis, 2 (4 %) patients were considered to be severe enough to warrant percutaneous coronary intervention. Calcified plaques, noncalcified plaques, and mixed plaques were detected in 40 (78.4 %), 14 (27.5 %), and 11 (21.6 %) patients, respectively. Next, to determine the indicators of the presence of obstructive coronary stenosis, the clinical characteristics were compared between HCM patients with and without obstructive coronary stenosis (Table 1). Diabetes was common among HCM patients with obstructive coronary stenosis (50.0 % vs 9.3 %, $P < 0.05$), and these patients also had a greater number of coronary risk factors (3.4 ± 0.9 vs 2.5 ± 1.1, $P < 0.05$) than those without obstructive stenosis. Hemoglobin A1c (HbA1c) levels tended to be higher in HCM patients with obstructive stenosis than in those without obstructive stenosis (6.3 ± 0.5 vs 5.9 ± 0.4, $P = 0.06$). The results of the analysis of indicators of obstructive coronary stenosis are shown in Table 3. In the univariate logistic regression analysis, diabetes and current smoking were found to be significantly correlated with obstructive stenosis. Multivariate logistic regression revealed that diabetes was an independent indicator of obstructive stenosis in patients with HCM (odds ratio, 10.00; 95 % confidence interval, 1.37–93.34; $P < 0.05$).

Cardiac morphology and function were analyzed in a total of 46 HCM patients, after the exclusion of 5 without

Table 2 Evaluation of coronary artery disease by cardiac computed tomography in patients with hypertrophic cardiomyopathy

	Total (n = 51)
Agatston score	
Mean score	198.8 ± 312.0
No. of patients with score:	
0	12 (23.5)
1–99	17 (33.3)
100–399	14 (27.5)
>400	8 (15.7)
No. of patients with coronary stenosis	
None	9 (17.6)
Nonobstructive stenosis	34 (66.7)
Obstructive stenosis	8 (15.7)
No. of patients with coronary plaques	
Calcified plaques	40 (78.4)
Noncalcified plaques	14 (27.5)
Mixed plaques	11 (21.6)

Vaues are mean ± standard deviation or number (%) of patients

Table 3 Indicators for obstructive coronary stenosis in patients with hypertrophic cardiomyopathy

	Odds ratio	95 % confidence interval	P value
Univariate analysis			
Advanced age	1.52	0.54–23.8	1.00
Men	5.54	0.63–49.0	0.09
Hypertension	1.38	0.29–6.67	0.68
Dyslipidemia	0.72	0.16–3.27	0.70
Diabetes mellitus	9.75	1.76–54.8	<0.005
Current smoking habits	6.83	0.80–58.0	<0.05
Multivariate analysis			
Men	6.41	0.84–146.4	0.08
Diabetes mellitus	10	1.37–93.3	<0.05
Current smoking habits	2.93	0.15–52.4	0.46

normal sinus rhythm (Table 4). LV outflow obstruction was detected in 5 (10.9 %) patients. Septal wall thickness and septum-to-lateral wall thickness ratios were significantly increased at 21.9 ± 5.7 mm and 2.4 ± 1.1, respectively. Maximal wall thickness was located in the apical wall in 7 (15.2 %), in the anterior free wall in 10 (21.7 %) patients, in the septal wall in 28 (60.9 %), and in the inferior wall in 1 (2.2 %). Hypertrophied right ventricular trabeculation in the interventricular septum and abnormal regional LV bulging were observed in 21 (45.7 %) and 14 (30.4 %) patients, respectively. Among the 46 analyzed patients,

Table 4 Evaluation of cardiac morphology and function by cardiac computed tomography in patients with hypertrophic cardiomyopathy

	Total (N = 46)
Septal wall thickness (mm)	21.9 ± 5.7
Septum-to-lateral wall thickness ratios	2.4 ± 1.1
Location of maximal wall thickness	
Anterior free wall	10 (21.7)
Septal wall	28 (60.9)
Inferior wall	1 (2.2)
LV obstruction	5 (10.9)
Hypertrophied right ventricular trabeculation in the interventricular septum	21 (45.7)
Abnormal regional LV bulging	14 (30.4)
LVEDV (ml)	128.5 ± 35.6
LVEDV index (ml/m^2)	78.6 ± 21.8
LVESV (ml)	43.6 ± 30.7
LVESV index (ml/m^2)	27.2 ± 20.7
LVEF (%)	67.9 ± 15.7
LV mass (g)	161.7 ± 58.7
LV mass index (g/m^2)	97.4 ± 28.9
LA volume (ml)	100.3 ± 34.7
LA volume index (ml/m^2)	61.5 ± 21.4

Values are mean ± standard deviation or number (%) of patients

LV left ventricular, *LVEDV* left ventricular end-diastolic volume, *LVESV* left ventricular end-systolic volume, *LVEF* left ventricular ejection fraction, *LA* left atrial

LVEF was preserved at 67.9 ± 15.7 %. The LV mass index and LA volume index, reflecting LV diastolic function, were considered to be elevated, at 97.4 ± 28.9 g/m^2 and 61.5 ± 21.4 ml/m^2, respectively, as opposed to the values reported in studies performed on normal subjects [28, 29]. The predictors of LV mass index were evaluated by an analysis that accounted for age; body mass index; systolic and diastolic blood pressure; levels of HbA1c, triglycerides, LDL-cholesterol, and B-type natriuretic peptide; estimated glomerular filtration rate; and Agatston score (Table 5). In the univariate linear regression analysis, the estimated glomerular filtration rate was significantly correlated with LV mass index (β, −0.51; standard error, 0.21; $P < 0.05$), whereas the body mass index and triglyceride levels showed a tendency to be associated only with LV mass index. Multivariate linear regression revealed that the low estimated glomerular filtration rate (β, −0.53; standard error, 0.17; $P < 0.01$) and high triglyceride concentrations (β, 0.16; standard error, 0.06; $P < 0.05$) were independent indicators of a high LV mass index.

Table 5 Indicators for left ventricular mass index in patients with hypertrophic cardiomyopathy

	β	Standard error	P value
Univariate analysis			
Age	−0.18	0.37	0.63
Body mass index	1.99	1.15	0.09
Systolic BP	0.27	0.22	0.23
Diastolic BP	0.39	0.35	0.27
HbA1c	−7.83	11.13	0.49
Triglycerides	0.13	0.078	0.09
LDL-C	0.22	0.17	0.21
eGFR	−0.51	0.21	<0.05
BNP	0.0091	0.018	0.62
Agatston score	0.015	0.014	0.29
Multivariate analysis			
Body mass index	1.24	1.11	0.27
Triglycerides	0.16	0.06	<0.05
eGFR	−0.53	0.17	<0.01

BP blood pressure, *HbA1c* hemoglobin A1c, *LDL-C* low-density lipoprotein cholesterol, *eGFR* estimated glomerular filtration rate, *BNP* B-type natriuretic peptide

Discussion

In the present study, coronary artery disease and cardiac morphology and function were evaluated in patients with HCM, using cardiac CT. In particular the study investigated the prevalence of coronary artery disease, the indicators of the presence of obstructive coronary stenosis, and the magnitude of LV hypertrophy. The prevalence of obstructive coronary stenosis was approximately 16 % in HCM patients without typical chest pain. Moreover, the coronary calcium scores were relatively high, and elevated according to the increase in the number of coronary risk factors. These results suggest that coronary artery disease is common among HCM patients, even without typical chest pain, and that the management of coronary risk factors is equally important for HCM patients and the general population.

In addition, a number of patients with HCM had non-calcified and/or mixed plaques, both of which are reported to be closely related to cardiovascular events. In a study on cardiac CT and intravascular ultrasonography by Pundziute et al. [30], noncalcified and mixed plaques were more commonly detected in patients with acute coronary syndrome than in those with stable coronary artery disease; they also noted that thin-cap fibroatheromas, which increased the risk of plaque rupture causing acute coronary syndrome, were frequently observed in patients with mixed plaques. With these observations in mind, we speculate that many HCM patients may undergo sudden cardiac death resulting from coronary artery disease rather than from arrhythmias. Further evaluation of the prognostic value of coronary artery disease in patients with HCM is thus required.

HCM patients with obstructive coronary stenosis commonly had diabetes, which was a significant predictor of the presence of obstructive stenosis in both the univariate and multivariate regression analyses. Diabetes is one of the important risk factors for coronary artery disease, and can often mask the symptoms of coronary artery disease due to autonomic denervation of the heart, resulting in delayed diagnosis [31]. Therefore, diabetic HCM patients should undergo screening tests, such as cardiac CT, for coronary artery disease.

A novel finding regarding cardiac morphology in HCM patients was that the low estimated glomerular filtration rates and high triglyceride concentrations were independent indicators of a high LV mass index. Other studies have shown that the magnitude of the LV hypertrophy is closely related to sudden cardiac death and poor prognosis in patients with HCM [32]; however, its indicators have not been sufficiently investigated. We believe that identification of the indicators of the magnitude of LV hypertrophy in HCM patients may provide useful information for prognostic evaluations. Renal dysfunction and hypertriglycemia have been reported to be associated with the magnitude of LV hypertrophy in studies not involving HCM patients. Park et al. [33] reported that renal dysfunction was closely associated with high LV mass indexes, even after adjusting for variables such as age, gender, anemia, albuminuria, detection of markers of mineral metabolism, hypertension, and diabetes. Schillaci et al. [34] also reported that hypertriglycemia was independently associated with high LV mass indexes after taking into account the effects of age, body mass index, blood pressure, and smoking in women. The results of these reports are similar to the present results. The precise mechanism(s) by which estimated glomerular filtration rate and triglycerides can predict the magnitude of LV hypertrophy in patients with HCM is open to further investigation.

Differentiating HCM from hypertensive heart disease is occasionally difficult. However, the present subjects had significantly increased septum-to-lateral wall thickness ratios, and any one of asymmetrical LV hypertrophy, hypertrophied right ventricular trabeculation in the interventricular septum, or abnormal regional LV bulging. These findings are characteristic of HCM [27], and we believe that HCM can be diagnosed clinically and morphologically, as accurately as possible, by differentiating it from hypertensive heart disease.

Limitations

Our study findings should be carefully interpreted in light of the following limitations. First, our study was retrospective, with small sample sizes, at two centers, and the prevalence of coronary artery disease can vary according to patient characteristics such as age, gender, and coronary risk factors. Second, the effects of coronary artery disease on the prognosis of patients with HCM could not be demonstrated because of the absence of follow-up data. Third, genetic diagnoses can more accurately diagnose HCM [35, 36], but could not be performed because of the retrospective nature of the study and high expenses associated with such diagnoses. Further investigations are thus required to overcome these limitations.

Conclusion

Coronary artery disease was common among patients with HCM. The presence of obstructive stenosis and the magnitude of LV hypertrophy were closely related to diabetes, triglyceride levels, and the estimated glomerular filtration rate. Cardiac CT can provide important information regarding coronary artery disease and cardiac morphology and function in patients with HCM.

References

1. Maron BJ (2002) Hypertrophic cardiomyopathy: a systematic review. JAMA 287:1308–1320
2. Elliott PM, Poloniecki J, Dickie S, Sharma S, Monserrat L, Varnava A, Mahon NG, McKenna WJ (2000) Sudden death in hypertrophic cardiomyopathy: identification of high risk patients. J Am Coll Cardiol 36:2212–2218
3. Maron BJ, Olivotto I, Spirito P, Casey SA, Bellone P, Gohman TE, Graham KJ, Burton DA, Cecchi F (2000) Epidemiology of hypertrophic cardiomyopathy-related death: revisited in a large non-referral-based patient population. Circulation 102:858–864
4. Melacini P, Basso C, Angelini A, Calore C, Bobbo F, Tokajuk B, Bellini N, Smaniotto G, Zucchetto M, Iliceto S, Thiene G, Maron BJ (2010) Clinicopathological profiles of progressive heart failure in hypertrophic cardiomyopathy. Eur Heart J 31:2111–2123
5. Olivotto I, Cecchi F, Casey SA, Dolara A, Traverse JH, Maron BJ (2001) Impact of atrial fibrillation on the clinical course of hypertrophic cardiomyopathy. Circulation 104:2517–2524
6. Sorajja P, Ommen SR, Nishimura RA, Gersh BJ, Berger PB, Tajik AJ (2003) Adverse prognosis of patients with hypertrophic cardiomyopathy who have epicardial coronary artery disease. Circulation 108:2342–2348
7. Ueda H, Harimoto K, Tomoyama S, Tamaru H, Miyawaki M, Mitsusada N, Yasuga Y, Hiraoka H (2012) Relation of cardiovascular risk factors and angina status to obstructive coronary artery disease according to categorical coronary artery calcium score. Heart Vessels 27:128–134
8. Soeda T, Uemura S, Okayama S, Kawakami R, Sugawara Y, Nakagawa H, Matsumoto T, Sung JH, Nishida T, Senoo A, Somekawa S, Takeda Y, Ishigami K, Kawata H, Horii M, Saito Y (2011) Intensive lipid-lowering therapy with rosuvastatin stabilizes lipid-rich coronary plaques. Evaluation using dual-source computed tomography. Circ J 75:2621–2627
9. Soeda T, Uemura S, Morikawa Y, Ishigami K, Okayama S, Hee SJ, Nishida T, Onoue K, Somekawa S, Takeda Y, Kawata H, Horii M, Saito Y (2011) Diagnostic accuracy of dual-source computed tomography in the characterization of coronary atherosclerotic plaques: comparison with intravascular optical coherence tomography. Int J Cardiol 148:313–318
10. Wu YW, Tadamura E, Kanao S, Yamamuro M, Okayama S, Ozasa N, Toma M, Kimura T, Kita T, Marui A, Komeda M, Togashi K (2008) Left ventricular functional analysis using 64-slice multidetector row computed tomography: comparison with left ventriculography and cardiovascular magnetic resonance. Cardiology 109:135–142
11. Hof I, Arbab-Zadeh A, Dong J, Scherr D, Chilukuri K, Calkins H (2008) Validation of a simplified method to determine left atrial volume by computed tomography in patients with atrial fibrillation. Am J Cardiol 102:1567–1570
12. Berliner JI, Kino A, Carr JC, Bonow RO, Choudhury L (2012) Cardiac computed tomographic imaging to evaluate myocardial scarring/fibrosis in patients with hypertrophic cardiomyopathy: a comparison with cardiac magnetic resonance imaging. Int J Cardiovasc Imaging 29:191–197
13. Ehara S, Matsumoto K, Shirai N, Nakanishi K, Otsuka K, Iguchi T, Hasegawa T, Nakata S, Yoshikawa J, Yoshiyama M (2013) Typical coronary appearance of dilated cardiomyopathy versus left ventricular concentric hypertrophy: coronary volumes measured by multislice computed tomography. Heart Vessels 28: 188–198
14. Zhao L, Ma X, Delano MC, Jiang T, Zhang C, Liu Y, Zhang Z (2012) Assessment of myocardial fibrosis and coronary arteries in hypertrophic cardiomyopathy using combined arterial and delayed enhanced CT: comparison with MR and coronary angiography. Eur Radiol 23:1034–1043
15. Martínez M, Castillo-Moreno JA, Pérez-Milá L, Cano-Vivar P (2010) Value of multidetector computed tomography in patients with chest pain and suspected apical hypertrophic cardiomyopathy. Rev Esp Cardiol 63:612–613
16. Chen CC, Chen MT, Lei MH, Hsu YC, Chung SL, Sung YJ (2010) Assessing myocardial bridging and left ventricular configuration by 64-slice computed tomography in patients with apical hypertrophic cardiomyopathy presenting with chest pain. J Comput Assist Tomogr 34:70–74
17. Okayama S, Uemura S, Soeda T, Horii M, Saito Y (2010) Role of cardiac computed tomography in planning and evaluating percutaneous transluminal septal myocardial ablation for hypertrophic obstructive cardiomyopathy. J Cardiovasc Comput Tomogr 4:62–65
18. Goldman L, Weinberg M, Weisberg M, Olshen R, Cook EF, Sargent RK, Lamas GA, Dennis C, Wilson C, Deckelbaum L, Fineberg H, Stiratelli R (1982) A computer-derived protocol to aid in the diagnosis of emergency room patients with acute chest pain. N Engl J Med 307:588–596
19. Okayama S, Uemura S, Saito Y (2013) Evaluation of epicardial and intra-myocardial fat in a patient with mitochondrial cardiomyopathy. Int J Cardiol 167:e43–e45
20. Maron MS, Olivotto I, Betocchi S, Casey SA, Lesser JR, Losi MA, Cecchi F, Maron BJ (2003) Effect of left ventricular outflow tract obstruction on clinical outcome in hypertrophic cardiomyopathy. N Engl J Med 348:295–303
21. Wang TJ (2008) New cardiovascular risk factors exist, but are they clinically useful? Eur Heart J 29:441–444
22. Imai E, Horio M, Nitta K, Yamagata K, Iseki K, Tsukamoto Y, Ito S, Makino H, Hishida A, Matsuo S (2007) Modification of the

modification of diet in renal disease (MDRD) study equation for Japan. Am J Kidney Dis 50:927–937
23. Lee J (2011) Coronary artery calcium scoring and its impact on the clinical practice in the era of multidetector CT. Int J Cardiovasc Imaging 27(Suppl 1):9–25
24. Austen WG, Edwards JE, Frye RL, Gensini GG, Gott VL, Griffith LS, McGoon DC, Murphy ML, Roe BB (1975) A reporting system on patients evaluated for coronary artery disease. Report of the Ad Hoc Committee for Grading of Coronary Artery Disease, Council on Cardiovascular Surgery, American Heart Association. Circulation 51:5–40
25. Cheng VY, Wolak A, Gutstein A, Gransar H, Wong ND, Dey D, Thomson LE, Hayes SW, Friedman JD, Slomka PJ, Berman DS (2010) Low-density lipoprotein and noncalcified coronary plaque composition in patients with newly diagnosed coronary artery disease on computed tomographic angiography. Am J Cardiol 105:761–766
26. Gao Y, Lu B, Sun ML, Hou ZH, Yu FF, Cao HL, Chen Y, Yang YJ, Jiang SL, Budoff MJ (2011) Comparison of atherosclerotic plaque by computed tomography angiography in patients with and without diabetes mellitus and with known or suspected coronary artery disease. Am J Cardiol 108:809–813
27. Sipola P, Magga J, Husso M, Jääskeläinen P, Peuhkurinen K, Kuusisto J (2011) Cardiac MRI assessed left ventricular hypertrophy in differentiating hypertensive heart disease from hypertrophic cardiomyopathy attributable to a sarcomeric gene mutation. Eur Radiol 21:1383–1389
28. Sandstede J, Lipke C, Beer M, Hofmann S, Pabst T, Kenn W, Neubauer S, Hahn D (2000) Age- and gender-specific differences in left and right ventricular cardiac function and mass determined by cine magnetic resonance imaging. Eur Radiol 10:438–442
29. Maceira AM, Cosín-Sales J, Roughton M, Prasad SK, Pennell DJ (2010) Reference left atrial dimensions and volumes by steady state free precession cardiovascular magnetic resonance. J Cardiovasc Magn Reson 12:65
30. Pundziute G, Schuijf JD, Jukema JW, Decramer I, Sarno G, Vanhoenacker PK, Boersma E, Reiber JH, Schalij MJ, Wijns W, Bax JJ (2008) Evaluation of plaque characteristics in acute coronary syndromes: non-invasive assessment with multi-slice computed tomography and invasive evaluation with intravascular ultrasound radiofrequency data analysis. Eur Heart J 29: 2373–2381
31. Niakan E, Harati Y, Rolak LA, Comstock JP, Rokey R (1986) Silent myocardial infarction and diabetic cardiovascular autonomic neuropathy. Arch Intern Med 146:2229–2230
32. Spirito P, Bellone P, Harris KM, Bernabo P, Bruzzi P, Maron BJ (2000) Magnitude of left ventricular hypertrophy and risk of sudden death in hypertrophic cardiomyopathy. N Engl J Med 342:1778–1785
33. Park M, Hsu CY, Li Y, Mishra RK, Keane M, Rosas SE, Dries D, Xie D, Chen J, He J, Anderson A, Go AS, Shlipak MG (2012) Associations between kidney function and subclinical cardiac abnormalities in CKD. J Am Soc Nephrol 23:1725–1734
34. Schillaci G, Pirro M, Pucci G, Mannarino MR, Gemelli F, Siepi D, Vaudo G, Mannarino E (2006) Different impact of the metabolic syndrome on left ventricular structure and function in hypertensive men and women. Hypertension 47:881–886
35. Kawashiri MA, Hayashi K, Konno T, Fujino N, Ino H, Yamagishi M (2013) Current perspectives in genetic cardiovascular disorders: from basic to clinical aspects. Heart Vessels. doi:10.1007/s00380-013-0391-5
36. Fujita E, Nakanishi T, Nishizawa T, Hagiwara N, Matsuoka R (2013) Mutations in the cardiac troponin T gene show various prognoses in Japanese patients with hypertrophic cardiomyopathy. Heart Vessels. doi:10.1007/s00380-013-0332-3

Accepted Manuscript

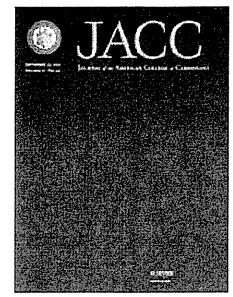

Does a ripple of Ca2+ leak develop into a rogue wave that can trigger pathological hypertrophy?

Masafumi Yano, Shinichi Okuda

PII: S0735-1097(13)06195-0

DOI: 10.1016/j.jacc.2013.10.064

Reference: JAC 19624

To appear in: *Journal of the American College of Cardiology*

Received Date: 2 October 2013

Revised Date: 25 October 2013

Accepted Date: 28 October 2013

Please cite this article as: Yano M, Okuda S, Does a ripple of Ca2+ leak develop into a rogue wave that can trigger pathological hypertrophy?, *Journal of the American College of Cardiology* (2013), doi: 10.1016/j.jacc.2013.10.064.

Does a ripple of Ca^{2+} leak develop into a rogue wave that can trigger pathological hypertrophy?

Running Title: Ca2+ leak and cardiac hypertrophy

Masafumi Yano*, Shinichi Okuda

Department of Medicine and Clinical Science, Division of Cardiology,
Yamaguchi University Graduate School of Medicine
1-1-1 Minamikogushi, Ube, Yamaguchi 755-8505, Japan

Word count: 1744

*Address for correspondence:
Masafumi Yano, M.D., Ph.D.
Department of Medicine and Clinical Science
Division of Cardiology
Yamaguchi University Graduate School of Medicine
1-1-1 Minamikogushi, Ube, Yamaguchi 755-8505, Japan
Tel: +81-836-22-2248; Fax: +81-836-22-2246; Email: yanoma@yamaguchi-u.ac.jp

There are no conflicts of interest to declare.

Key Words: calcium, remodeling, hypertension, heart failure, ryanodine receptor